# PNAS

## www.pnas.org

**Supplementary Information for**

**S-Nitrosylated TDP-43 triggers aggregation, cell-to-cell spread, and neurotoxicity in hiPSC- and in vivo-models of ALS/FTD**

Elaine Pirie[1], Chang-ki Oh[1], Xu Zhang, Xuemei Han, Piotr Cieplak, Henry R. Scott, Amanda K. Deal, Swagata Ghatak, Fernando J. Martinez, Gene W. Yeo, John R. Yates, III, Tomohiro Nakamura[*], and Stuart A. Lipton[*]


[1]E.P. and C.O. contributed equally to this work.

[*]To whom correspondence may be addressed. Email: tnakamura@scripps.edu or slipton@scripps.edu.

**This PDF file includes:**
      Supplementary text (Materials and Methods)
      Figures S1 to S5
      Tables S1
      SI References

**Supplementary information text**

**Materials and Methods**

**Stereotaxic Surgery and Quantitative Immunohistochemistry.** All animal experiments were performed in accordance with the guidelines outlined by the Institutional Animal Care and Use Committees at The Scripps Research Institute. WT C57/B6 mice at the age of 3 months received bilateral, stereotactic injections of recombinant TDP-43(1-265) (1 µg) with or without L-NAME (2 µg) into the cortex at a rate of 1 µl per 2 min for a total of 2 µl into each hemisphere. Tris-buffered saline was used for vehicle/control injections. Coordinates used for the injection were as follows (1): AP-2.5, ML±2, and DV-0.8. Four weeks after TDP-43 injection, mice were anesthetized, perfused transcardially with PBS, followed by 4% PFA perfusion. Brains were then removed and fixed in 4% PFA for 72 h at 4 °C and kept in 1% PFA until analyzed. Quantitative immunohistochemical analysis was performed using free-floating, 40 µm-thick, vibratome-cut, blind-coded sections, as described previously (2-4). Immunolabeling was performed using antibodies against phospho(409/410)-TDP-43 (Proteintech, 22309-1-AP), pCREB (Ser133) (87G3) (Cell Signaling Technology, #9198), CREB (Santa Cruz Biotechnology, sc-374227), NeuN (Abcam, ab104224), and MAP2 (Sigma, M4403). For each section, a total of three to four digital images were obtained from the cortex adjacent to the injection site using an A1 Confocal Laser microscope (Nikon). Quantification of pCREB and MAP2 immunoreactivity was determined with FIJI (ImageJ) software as described (2, 5).

**Chemicals and Reagents.** All reagents were obtained from Sigma unless otherwise stated. The physiological NO donors, SNOC and GSNO were prepared as described previously (6, 7). Hydrogen peroxide was obtained from Millipore. The calcium ionophore A23187 was purchased from Thermo Fisher Scientific, and the NOS inhibitor L-NAME from Enzo Life Sciences. Antibodies used for immunoblots in this study included anti-ND3 antibody (Abcam ab170681), anti-ND6 antibody (Santa Cruz SC-20667), anti-GAPDH antibody (Millipore, MAB374, clone 6C5), anti-V5 (Thermo Fisher Scientific, R960-25), anti-TDP-43 antibody (Proteintech, #10782-2-AP), and anti-actin antibody (EMD Millipore, #mab1501).

**Plasmid Constructs and siRNAs.** Human TDP-43 cDNA with N-terminal V5 tag was cloned into pcDNA3.1. Point mutations were introduced by the QuikChange Lightning Mutagenesis Kit (Agilent Technologies) or the In-Fusion HD Cloning Plus kit (Takara Bio). siRNAs targeting TDP-43 (#4392420) and control (#4390843) sequence were purchased from Ambion｜Thermo Fisher Scientific. For bacterial expression of N-terminal TDP-43 (encoding amino acids 1 to 265), the corresponding region of TDP-43 cDNA was inserted into pET28a to provide a His-tag.

**Detection of S-Nitrosylated TDP-43 (SNO-TDP-43).** The biotin-switch assay for the detection of exogenous SNO-TDP-43 was performed as previously described with minor modifications (8-10). In brief, cells or tissues were lysed in HENTS buffer (100 mM Hepes, 1 mM EDTA, 0.1 mM neocuproine, pH7.4, 1% Triton X-100, and 0.1% SDS), followed by centrifugation at 12,000 rpm at 4 °C. Supernatants from lysates were

mixed with 4 volumes of blocking buffer [2.5% SDS and 10 mM methyl methanethiosulfonate (MMTS) in HEN buffer], and incubated at 42 °C for 20 min to block free thiols. Excess MMTS was removed by acetone precipitation, and the samples were incubated with 20 mM ascorbate and 1 mM biotin-HPDP (*N*-[6-(biotinamido)-hexyl]-1'-(2'pyridyldithio) propionamide [Dojindo]) for 1 h at room temperature. After acetone precipitation, the biotinylated proteins were collected by High Capacity NeutrAvidin Agarose (Thermo Fisher Scientific). The pulled-down proteins were separated on a 4-12% NuPAGE Bis-Tris gel (Thermo Fisher Scientific) and transferred to an Immobilon-FL PVDF membrane (EMD Millipore). TDP-43 and actin were detected with rabbit polyclonal anti-TDP-43 antibody (Proteintech, #10782-2-AP) and mouse monoclonal anti-actin antibody (EMD Millipore, #mab1501), respectively.

For the detection of endogenously produced SNO-TDP-43, cell or tissue lysates were prepared in HENTS buffer, followed by the addition of SDS (final concentration 1%) and MMTS (final concentration 10 mM) into the homogenates. Free thiols were blocked by MMTS incubation at 42 °C for 20 min. Genomic DNA and excess MMTS were removed by passing through Zeba Spin columns (Thermo Fisher Scientific), and proteins were precipitated by acetone before incubation with ascorbate and biotin-HPDP.

For quantification of immunoblots, all images were scanned with a LICOR Odyssey IR imaging system under non-saturating conditions. Identical regions were selected for each band in each lane for quantification of pixel intensity. Prior to quantitative analysis, all bands in the immunoblots were normalized against the corresponding loading control for each lane.

**Purification of Recombinant TDP-43(1-265).** Transformed BL21 (DE3) *E. coli* were grown in 2XYT medium to yield an absorbance A600 of 0.7, at which time 1 mM IPTG was added for 16 h. *E. coli* were harvested by centrifugation and resuspended in buffer containing 20 mM HEPES (pH 7.5), 1M NaCl, 10% glycerol, 30 mM imidazole, and 5 mM 2-mercaptoethanol. After sonication and centrifugation, recombinant TDP-43(1-265) protein was purified using TALON metal affinity resin (Takara) for 1 h at room temperature. The resin was washed 3 times with Tris buffer (50 mM Tris-HCl, pH 7.4; 150 mM NaCl), and the protein was eluted with 50 mM imidazole in TBS buffer. Excess imidazole was removed by PD-10 columns (GE Healthcare Life Sciences).

**Top-Down Mass Spectrometry.** Top-down mass spectrometry analysis of S-nitrosylated TDP-43 was performed as we previously described(9, 11). In brief, measurements were performed on an Orbitrap Fusion mass spectrometer (Thermo Electron) in the positive ion mode. Recombinant TDP-43(1-265) was mixed with 100 $\mu$M SNOC and then incubated for 20 min at room temperature. The samples were dissolved in buffer containing 50% methanol and 0.5% formic acid immediately before analysis. Sample concentration was 100 fmol/µl. Samples were delivered to the mass spectrometer through an ESI source using a syringe pump at a flow rate of 5 µl/min. Molecular weight and charge state of the proteins were deconvoluted from the multiply-charged peak envelope.

**Soluble and Insoluble Fractionation.** RIPA buffer (50 mM Tris pH 8.0, 150 mM NaCl, 1% NP-40, 5 mM EDTA, 0.5% sodium deoxycholate, 0.1% SDS) soluble and insoluble fractions were prepared from SH-SY5Y cells and hiPSC-derived motor neurons, as previously described (12). In brief, samples were mechanically separated by 4 passages through a 25-gauge needle, and then centrifuged for 10 min. After washing the resulting insoluble pellet in RIPA buffer, the sample was re-suspended in urea buffer (8 M urea, 1% Triton X-100 in PBS) to obtain the RIPA-insoluble fraction.

**Immunocytochemistry and TUNEL.** Immunocytochemistry experiments were conducted using SH-SY5Y cells grown on fibronectin (Thermo Fisher Scientific)-coated glass coverslips as previously described(9). In brief, cells were fixed in 4% paraformaldehyde in PBS for 10 min, and then permeabilized with 0.3% Triton X-100 in PBS. The following antibodies were employed: TDP-43 (Proteintech,10782-2-AP), G3BP (Abcam, ab56574), and Alexa 488 or 594-labelled secondary antibodies (Thermo Fisher Scientific, A11008 or A21422, respectively). Samples were mounted using Vectashield antifade mounting medium (Vector Laboratories). Acquisition of images was performed with an epifluorescence deconvolution microscope (Zeiss with Intelligent Imaging, Inc. software), ImageXpress Micro Confocal High-Content Imaging System (Molecular Devices), or A1 Confocal Laser microscope (Nikon). To detect cell death, in conjunction with condensed nuclear morphology, TUNEL assays were performed using the Click-iT® TUNEL Alexa Fluor® 488 Imaging Assay (Thermo Fisher Scientific) according to manufacturer's directions.

**Molecular Dynamics Simulations of TDP-43 Structure.** We performed a series of molecular dynamics simulations of 500 ns duration for TDP-43 with and without formation of a disulfide bond between Cys173 and Cys175. All simulations were initiated from the NMR structure (pdbid: 4BS2)(13) containing the RRM1 and RRM2 subdomains bound to an RNA fragment. Simulations were conducted with the GPU version of the pmemd module from the AMBER14 simulation package (14) in an explicit TIP3P water model enclosed in a truncated octahedron periodic box (15). A ff14SB force field was used (16). An appropriate number of counterions was added to make the entire simulated system neutral. A particle mesh Ewald method was employed to treat electrostatic interactions (17), and a 2fs time step was applied to conduct molecular dynamics simulations.

**Quantitative RT-PCR of mRNA.** RNA was prepared from cell lysates using MirVana (Thermo Fisher Scientific), and cDNA was synthesized using the SuperScript III first-strand synthesis system (Thermo Fisher Scientific) according to the manufacturer's protocol. Quantitative (q)RT-PCR was carried out using a Roche LC480 PCR System with SYBR Green. The q-RT-PCR conditions used were as follows: 95 °C for 10 min, followed by 40 cycles of denaturing at 95 °C for 15 s, and annealing/extension at 60 °C for 1 min in a 20 μl reaction volume. All primers for qRT–PCR were from Integrated DNA Technologies. The primers used were -- HDAC6 forward: CGCACAGGGCTGGTCTATG, HDAC6 reverse: TGGTGGCTGTCCCACAAGTT. Ribosomal 18S was used as a reference gene (5).

For mitochondrial ND3 mRNA analysis, mitochondria were isolated from SH-SY5Y cells transfected with WT or C173/175A mutant TDP-43-V5 using the Mitochondria Isolation Kit for Cultured Cells (Thermo Fisher Scientific) according to the manufacturer's protocol. Isolated mitochondria were lysed in immunoprecipitation lysis buffer (50 mM Tris, pH 7.4, 250 mM NaCl, 5 mM EDTA, 50 mM NaF, 1 mM $Na_3VO_4$, 1% Nonidet P40) containing 1X protease inhibitor cocktail (Thermo Fisher Scientific) and 100 U/ml RNase Inhibitor (Promega). Mitochondrial lysates were incubated with anti-TDP-43 antibody conjugated to magnetic beads overnight at 4 °C. Magnetic beads were then washed with lysis buffer, and RNAs were extracted using a Quick-RNA MiniPrep Plus kit (Zymo Research). Total RNA from SH-SY5Y cells expressing WT or C173/175A mutant TDP-43-V5 was extracted to normalize the amount of mitochondrial RNA. cDNA was synthesized using a QuantiTect Reverse Transcription Kit (Qiagen). The q-RT-PCR conditions used were as follows: 95 °C for 5 min, followed by 45 cycles of denaturing at 95 °C for 20 s, annealing 57 °C for 20 sec, and extension at 72 °C for 30 sec in a 20 μl reaction volume. The primers used were -- ND3 forward: CCCTTACGAGTGCGGCTTC, and ND3 reverse: AGTGGCAGGTTAGTTGTTTGTAGG.

**Cryptic Exon Assay.** Total RNA was extracted from SH-SY5Y cells using a Quick-RNA MiniPrep Plus kit (Zymo Research), and cDNA was synthesized using a QuantiTect Reverse Transcription Kit (Qiagen). Cryptic exons in ATG4B were amplified using previously described primers (18, 19). The PCR reactions were performed with Platinum® PCR SuperMix (Thermo Fisher Scientific) using the following protocol: 95 °C for 2 min, followed by 46 cycles of denaturing at 98 °C for 15 s, annealing at 63 °C for

15 s, extension at 72 °C for 30 s, and then final extension at 72 °C for an additional 7 min. PCR products were resolved by 1.5% agarose gel electrophoresis and detected with SYBR® Gold Nucleic Acid Gel Stain (Thermo Fisher Scientific). Expression of ribosomal 18S was measured as an internal control using qRT-PCR as described above.

For the detection of STMNT2 cryptic exon, total RNA from SH-SY5Y cells transfected with siControl or siTDP-43 siRNAs, or exposed to recombinant TDP-43 (200 nM), was extracted using a Quick-RNA MiniPrep Plus kit (Zymo Research). After cDNA synthesis using a QuantiTect Reverse Transcription Kit (Qiagen), STMN2 cryptic exon was amplified using previously described primers and techniques (20) with minor modifications. The standard RT-PCR reactions were performed with Platinum® PCR SuperMix (Thermo Fisher Scientific) using the following protocol: 95 °C for 5 min, followed by 43 cycles of denaturing at 95 °C for 30 s, annealing at 55 °C for 30 s, and extension at 68 °C for 20 s, and then final extension at 68 °C for an additional 10 min. PCR products were resolved by 1.5% agarose gel electrophoresis and detected with ethidium bromide. GAPDH was used as a reference gene. The primers used were – STMN2 exon 1 (forward): GACTCAGTGCCTTATTCAGT, STMN2 exon 2a (reverse): TTTCTCTCGAAGGTCTTCTG, GAPDH forward: ACCACAGTCCATGCCATCAC, and GAPDH reverse: TCCACCACCCTGTTGCTGTA. Quantitative (q)RT-PCR of STMNT2 cryptic exon was carried out using a Roche LC480 PCR System with SYBR Green. The following qRT-PCR conditions were used: 95 °C for 5 min, followed by 50 cycles of denaturing at 95 °C for 20 s, annealing 57 °C for 20 sec, and extension at 72 °C for 30 sec in a 20 µl reaction. The primers used were – truncated STMN2 RNA (forward):

GGACTCGGCAGAAGACCTTC, and truncated STMN2 RNA (reverse):

GCAGGCTGTCTGTCTCTCTC.

**Detection of NO-Related Species by DAF-FM and Griess Assays.** For DAF-FM

assay, rat primary cortical neurons were incubated with 50 nM TDP-43(1-265) protein

for 16 h, and then washed 3 times in PBS. Cells were loaded with 2.5 μM DAF-FM

diacetate (Thermo Fisher Scientific) in artificial cerebrospinal fluid (ACSF; 119 mM

NaCl, 26.2 mM $NaHCO_3$, 2.5 mM KCl, 1 mM $NaH_2PO_4$, 1.3 mM $MgCl_2$, and 10 mM

glucose) for 15 min at room temperature in the dark. After 2 washes with ACSF,

fluorescence was monitored as previously described (21). The Griess reagent assay for

nitrite and nitrate was performed on SH-SY5Y cell culture media as previously
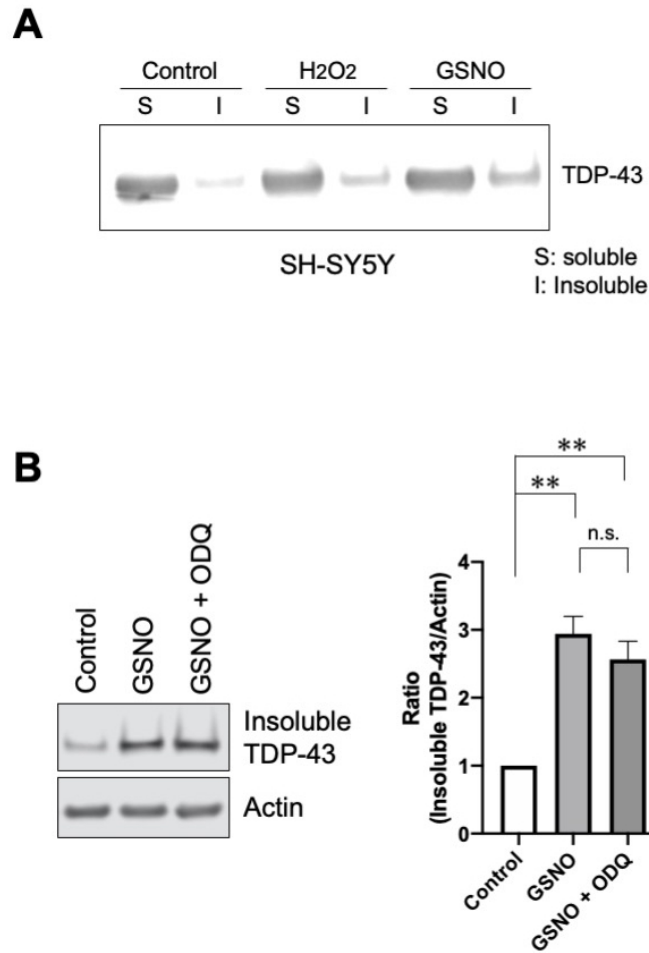
described (22).

**Fig. S1.** Nitrosative stress increases insoluble TDP-43. (*A*) SH-SY5Y cells were

exposed to 200 $\mu$M GSNO or $H_2O_2$, rested for 1 h, and fractionated in RIPA buffer into

soluble (S) and insoluble (I) fractions. Antibody against TDP-43 was used for

immunoblotting. (*B*) SH-SY5Y cells were pre-treated with or without 50 $\mu$M ODQ for 30

min and then exposed to 200 $\mu$M GSNO. *Left*: One hour after addition of GSNO, RIPA

soluble and insoluble fractions were analyzed by immunoblot. *Right*: Quantification of

insoluble TDP-43 levels (*n* = 3). Graph indicates mean + SEM; **$P < 0.01$ by one-way
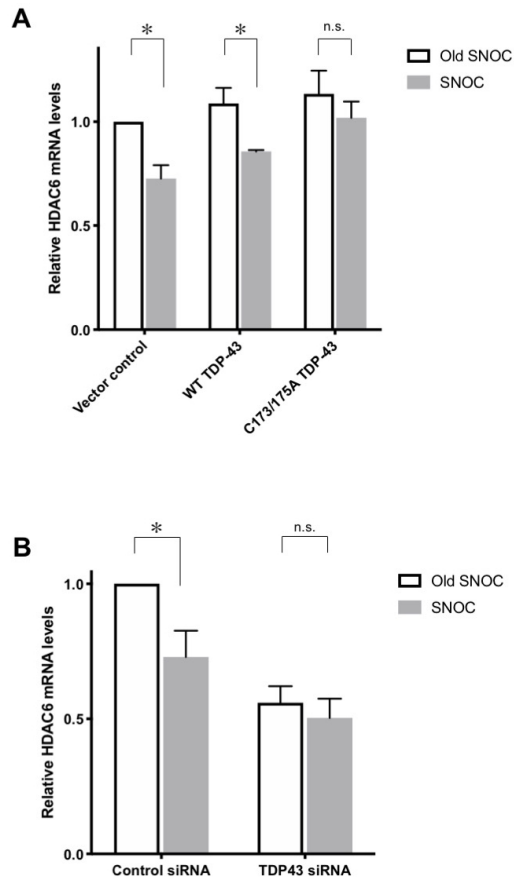
ANOVA, followed by Bonferroni's post-hoc test.

**Fig. S2.** Effects of SNOC on HDAC6 mRNA expression. (*A*) Non-nitrosylatable TDP-43(C173A/C175A) prevents SNOC-induced downregulation of HDAC6. SH-SY5Y cells were transfected with expression vectors encoding TDP-43 (WT or non-nitrosylatable C173A/C175A mutant). Empty vector (pcDNA3.1)-transfected SH-SY5Y cells served as a transfection control (Vector control). Cells were exposed to SNOC (200 μM), and after 13 h, HDAC6 mRNA levels were determined by qRT-PCR (*n* = 3). (*B*) siRNA-mediated knockdown of TDP-43 prevents further decrease of HDAC6 mRNA levels after exposure to SNOC (*n* = 3). Bars represent mean + SEM; *$P$ = 0.0131 (*A*, vector control, Old SNOC vs. SNOC), 0.0373 (*A*, WT TDP-43, Old SNOC vs. SNOC) and 0.0498 (*B*) by two-tailed Student's t test.
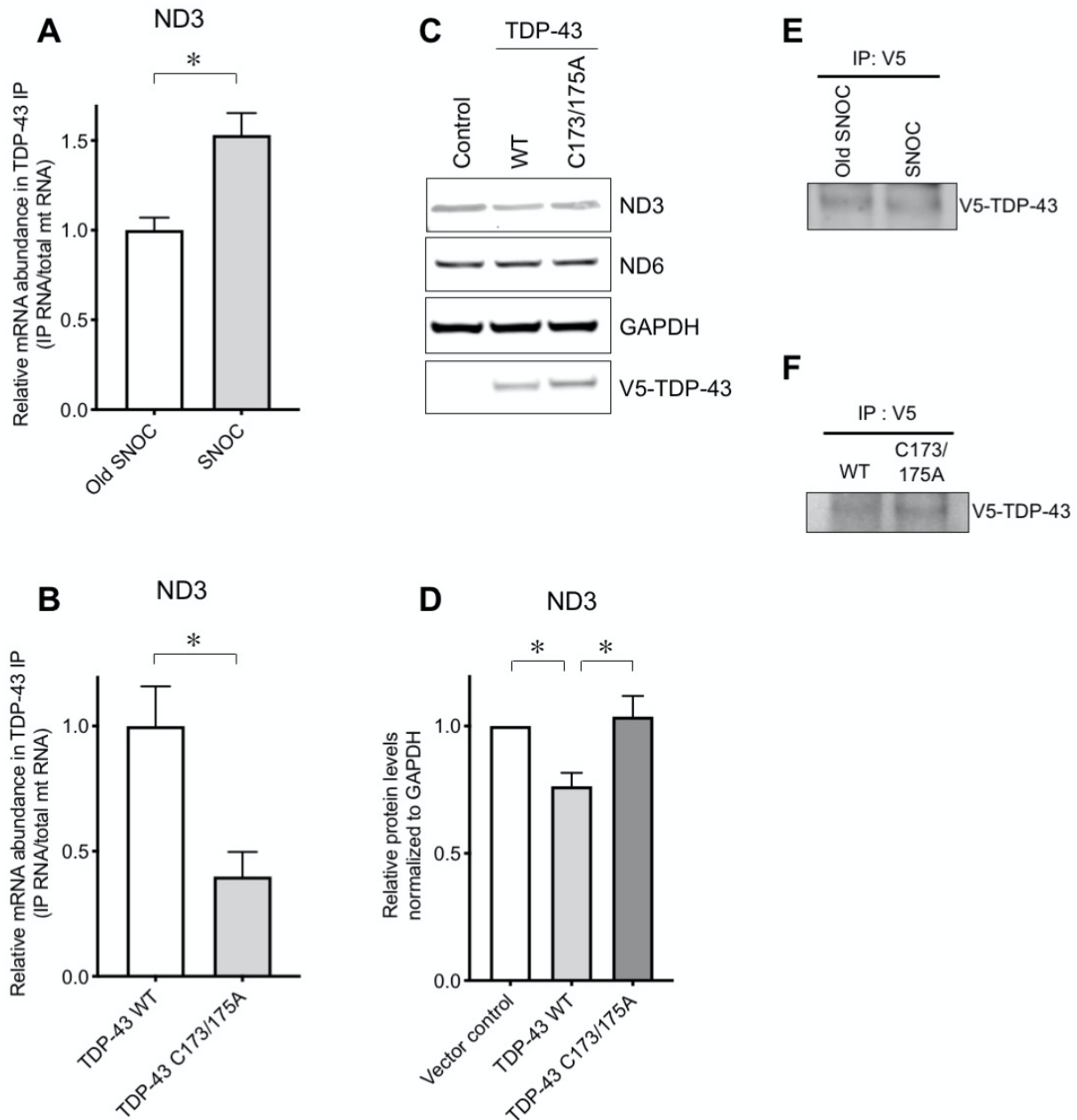
**Fig. S3.** Non-nitrosylatable mutant TDP-43 rescues decreased translation of mitochondrial complex I subunit ND3. (*A* and *B*) qRT-PCR analysis (*n* = 4) of mitochondrial ND3 mRNA in TDP-43 immunocomplexes prepared from SH-SY5Y mitochondrial fractions. (*C* and *D*) Immunoblots (*C*) and quantification (*D*) of ND3 protein expressed in SH-SY5Y cells (*n* = 4). Under the conditions of TDP-43

overexpression, endogenous NO increased so SNOC was not added (*B-D*). Bars represent mean + SEM; *P = 0.0092 (*A*), 0.0180 (*B*), 0.0043 (*C*, Vector control vs. TDP-43 WT), and 0.0307 (*C*, TDP-43 WT vs. TDP-43 C173/175A) by two-tailed Student's *t* test. (*E* and *F*) TDP-43 immunoprecipitation (IP) from mitochondrial fraction of SH-SY5Y cells. SH-SY5Y cells were transfected with V5-tagged WT TDP-43 or TDP-43(C173A/C175A). Equal levels of V5-tagged TDP-43 were subsequently immunoprecipitated from the mitochondrial fraction. Anti-V5 was used for immunoprecipitation and immunoblotting.
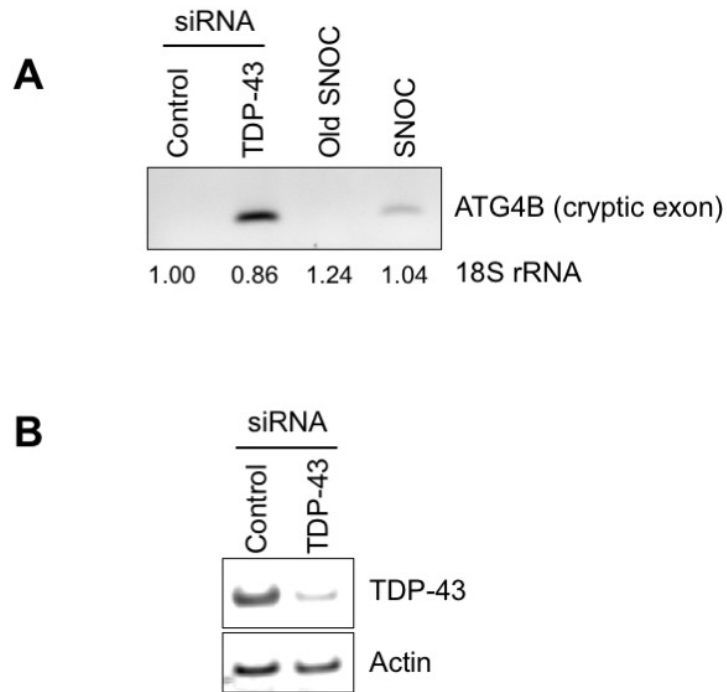
**Fig. S4.** Effects of SNOC on expression of the ATG4B cryptic exon. (*A*) *Top:* NO increases expression of the ATG4B cryptic exon, similar to knockdown of TDP-43 expression. *Bottom:* 18S rRNA levels were measured by qRT-PCR for internal standard. (*B*) Verification of siRNA-mediated TDP-43 knockdown in SH-SY5Y cells by immunoblot.
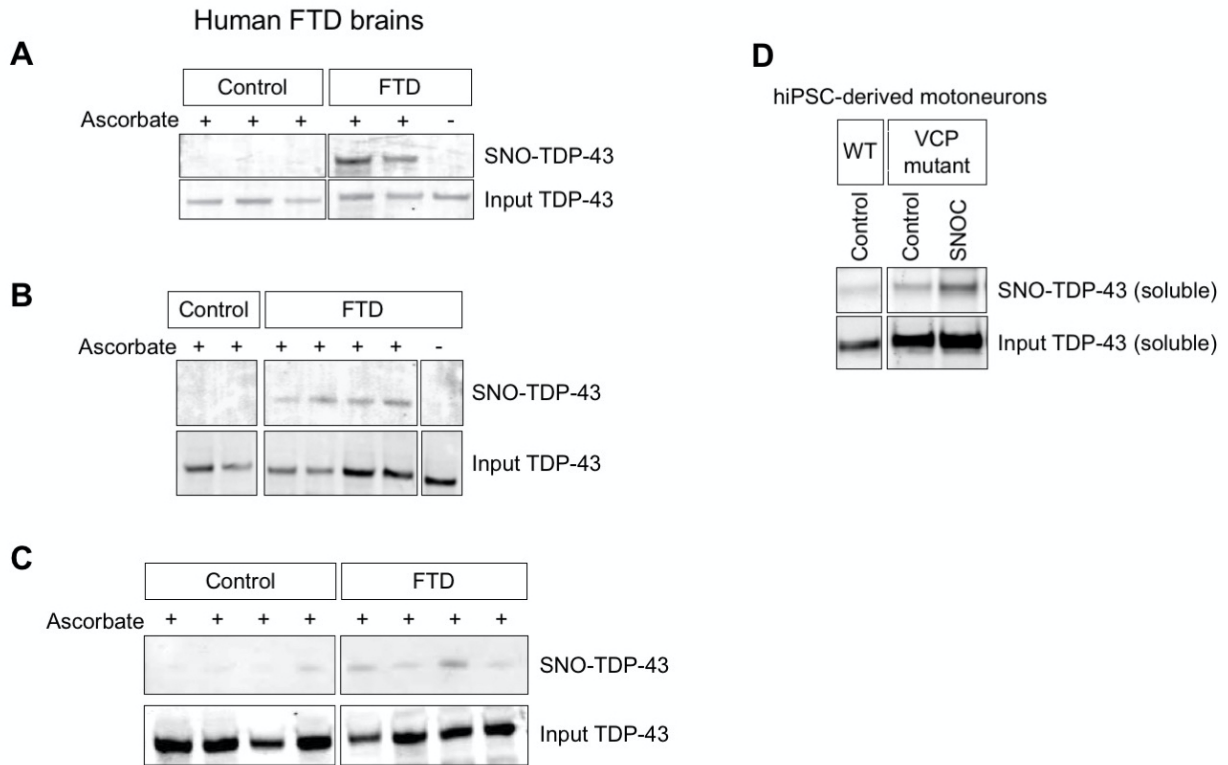
**Fig. S5.** S-Nitrosylation of TDP-43 in human FTD brains and hiPSC-derived motoneurons. (*A-C*) The biotin-switch assay detected increased SNO-TDP-43 levels in nearly all postmortem human FTD brain samples compared to control brains. Lack of ascorbate (-Asc) served as a negative control. Quantification of all samples is shown in Fig. 6*A* (*right-hand* panel). (*D*) Detection of SNO-TDP-43 in motor neurons derived from hiPSCs. hiPSCs carrying a mutation in the VCP gene were differentiated into motor neurons and exposed to 100 µM SNOC.

**Table S1.** List of human brains and diagnoses used this study.

| | Diagnosis | Age | Gender | Brain region | PMI |
|---|---|---|---|---|---|
| Control | | 87 | M | FC | N/A |
| Control | | 94 | M | FC | 12 |
| Control | | 80 | F | FC | 12 |
| Control | | 93 | F | FC | 18 |
| Control | | 97 | F | FC | 12 |
| Control | | 102 | F | FC | 9 |
| Control | | 91 | M | FC | 6 |
| Control | | 76 | M | FC | N/A |
| Control | | 63 | F | FC | 8 |
| | | | | | |
| Patient | FTD | 93 | M | FC | N/A |
| Patient | FTD | 69 | M | FC | N/A |
| Patient | FTD* | N/A | F | FC | 11 |
| Patient | FTD* | 68 | M | FC | 6 |
| Patient | FTD | 87 | M | FC | 12 |
| Patient | FTD* | 87 | F | FC | 6 |
| Patient | FTD | 72 | M | FC | 6 |
| Patient | FTD | 85 | M | FC | 12 |
| Patient | FTD* | 82 | M | FC | 15 |
| Patient | FTD* | 74 | F | FC | 6 |
| Patient | FTD | 60 | M | FC | 8 |
| Patient | FTD | 79 | F | FC | N/A |
| Patient | FTD* | 71 | F | FC | N/A |

M: male, F: female, FC: frontal cortex, FTD: Frontotemporal dementia, PMI: postmortem time in hours. *FTD patients with minor comorbid neurological conditions.

**SI References**

1.  S. Porta *et al.*, Patient-derived frontotemporal lobar degeneration brain extracts induce formation and spreading of TDP-43 pathology in vivo. *Nat. Commun.* **9**, 4220 (2018).
2.  S. A. Lipton *et al.*, Therapeutic advantage of pro-electrophilic drugs to activate the Nrf2/ARE pathway in Alzheimer's disease models. *Cell Death Dis.* **7**, e2499 (2016).
3.  M. Talantova *et al.*, Aβ induces astrocytic glutamate release, extrasynaptic NMDA receptor activation, and synaptic loss. *Proc. Natl. Acad. Sci. USA* **110**, E2518-2527 (2013).
4.  B. Spencer *et al.*, Reducing endogenous α-synuclein mitigates the degeneration of selective neuronal populations in an Alzheimer's disease transgenic mouse model. *J. Neurosci.* **36**, 7971-7984 (2016).
5.  S. Tu *et al.*, NitroSynapsin therapy for a mouse MEF2C haploinsufficiency model of human autism. *Nat. Commun.* **8**, 1488 (2017).
6.  B. Gaston *et al.*, Endogenous nitrogen oxides and bronchodilator S-nitrosothiols in human airways. *Proc. Natl. Acad. Sci. USA* **90**, 10957-10961 (1993).
7.  S. Z. Lei *et al.*, Effect of nitric oxide production on the redox modulatory site of the NMDA receptor-channel complex. *Neuron* **8**, 1087-1099 (1992).
8.  T. Uehara *et al.*, S-Nitrosylated protein-disulphide isomerase links protein misfolding to neurodegeneration. *Nature* **441**, 513-517 (2006).
9.  T. Nakamura *et al.*, Transnitrosylation of XIAP regulates caspase-dependent neuronal cell death. *Mol. Cell* **39**, 184-195 (2010).
10. S. R. Jaffrey, H. Erdjument-Bromage, C. D. Ferris, P. Tempst, S. H. Snyder, Protein S-nitrosylation: a physiological signal for neuronal nitric oxide. *Nat. Cell Biol.* **3**, 193-197 (2001).
11. S. Okamoto *et al.*, S-Nitrosylation-mediated redox transcriptional switch modulates neurogenesis and neuronal cell death. *Cell Rep.* **8**, 217-228 (2014).
12. T. J. Cohen, A. W. Hwang, T. Unger, J. Q. Trojanowski, V. M. Lee, Redox signalling directly regulates TDP-43 via cysteine oxidation and disulphide cross-linking. *EMBO J.* **31**, 1241-1252 (2012).
13. P. J. Lukavsky *et al.*, Molecular basis of UG-rich RNA recognition by the human splicing factor TDP-43. *Nat. Struct. Mol. Biol.* **20**, 1443-1449 (2013).
14. R. Salomon-Ferrer, A. W. Gotz, D. Poole, S. Le Grand, R. C. Walker, Routine microsecond molecular dynamics simulations with AMBER on GPUs. 2. Explicit solvent particle mesh Ewald. *J. Chem. Theory Comput.* **9**, 3878-3888 (2013).
15. W. L. Jorgensen, J. Chandrasekhar, J. D. Madura, Comparison of simple potential functions for simulating liquid water. *J. Chem. Phys.* **79**, 926-935 (1983).
16. J. A. Maier *et al.*, ff14SB: Improving the accuracy of protein side chain and backbone parameters from ff99SB. *J. Chem. Theory Comput.* **11**, 3696-3713 (2015).
17. T. Darden, D. York, L. Pedersen, Particle mesh Ewald: an nlog(n) method for Ewald sums in large systems. *J. Chem. Phys.* **98**, 10089–10092 (1993).

18. J. P. Ling, O. Pletnikova, J. C. Troncoso, P. C. Wong, TDP-43 repression of nonconserved cryptic exons is compromised in ALS-FTD. *Science* **349**, 650-655 (2015).
19. M. Sun *et al.*, Cryptic exon incorporation occurs in Alzheimer's brain lacking TDP-43 inclusion but exhibiting nuclear clearance of TDP-43. *Acta Neuropathol.* **133**, 923-931 (2017).
20. Z. Melamed *et al.*, Premature polyadenylation-mediated loss of stathmin-2 is a hallmark of TDP-43-dependent neurodegeneration. *Nat. Neurosci.* **22**, 180-190 (2019).
21. S. D. Ryan *et al.*, Isogenic human iPSC Parkinson's model shows nitrosative stress-induced dysfunction in MEF2-PGC1α transcription. *Cell* **155**, 1351-1364 (2013).
22. D. A. Wink *et al.*, Detection of S-nitrosothiols by fluorometric and colorimetric methods. *Methods Enzymol.* **301**, 201-211 (1999).